Dipole dynamics of an interacting bosonic mixture

Luca Cavicchioli [1,2] Chiara Fort [1,2] Michele Modugno [3,4,5] Francesco Minardi [1,2,6] and Alessia Burchianti [1,2,*]

[1]*Istituto Nazionale di Ottica, CNR-INO, 50019 Sesto Fiorentino, Italy*
[2]*LENS and Dipartimento di Fisica e Astronomia, Università di Firenze, 50019 Sesto Fiorentino, Italy*
[3]*Department of Physics, University of the Basque Country UPV/EHU, 48080 Bilbao, Spain*
[4]*IKERBASQUE, Basque Foundation for Science, 48013 Bilbao, Spain*
[5]*EHU Quantum Center, University of the Basque Country UPV/EHU, Leioa, 48940 Biscay, Spain*
[6]*Dipartimento di Fisica e Astronomia, Università di Bologna, 40127 Bologna, Italy*

We unravel the coupled dipole dynamics of a two-species Bose-Einstein condensate with tunable interspecies interaction. We produce a degenerate mixture of ^{41}K - ^{87}Rb in an optical trap and we study the dipole oscillations of both atomic species in the linear response regime. Varying the interspecies interaction from the weakly to the strongly attractive side, we measure the frequencies and the composition of the two dipole eigenmodes. For sufficiently strong interactions, even beyond the mean-field collapse, we find that the frequency of the low-energy eigenmode is determined only by the bare trap frequencies and the species population imbalance. The experimental results are well reproduced by numerical simulations based on two coupled Gross-Pitaevskii equations. Our findings provide a detailed picture of the dipole excitations in asymmetric bosonic mixtures.

I. INTRODUCTION

Multicomponent quantum systems emerge in a variety of physical contexts ranging from condensed matter to cosmology. In multicomponent superfluids, the interactions among constituents give rise to a number of fascinating and still not fully understood phenomena, which may be relevant in superconductors [1–4], liquid helium [5,6], and neutron stars [7–9]. Quantum degenerate atomic mixtures have proven to be ideal platforms to study multicomponent superfluidity [10–12], thanks to the high control and tunability offered by ultracold gases experiments.

Superfluidity in mixtures drastically differs from the single-component case [13,14] because of its critical dependence on the system's excitation spectrum. In the context of ultracold gases, the collective excitations of two-component superfluids confined in an external potential have been studied both theoretically [15–17] and experimentally, with internal states [18–21] and with different atomic species [10–12,22].

The dipole mode is the most basic example of collective oscillations: in a single-component superfluid trapped in a harmonic potential, it corresponds to rigid oscillations of the density, whose frequency, equal to the corresponding harmonic value, is independent of the interatomic interac-

tions [23]. For two interacting superfluids, this simple picture is no longer valid since the mutual interaction mixes the dipole modes of the two components and shifts their frequencies. Thus, in this case, the study of dipole dynamics allows access to the intercomponent interaction [12,20] and may provide insights into the nature of superfluidity [11,24]. The experimental realization of binary mixtures of Fermi-Bose superfluids [11,12,25] has renewed interest in the study of collective oscillations [26–31]. Conversely, the excitation spectrum of Bose-Bose mixtures has remained relatively unexplored and the experiments have mainly focused on either symmetric spin mixtures [18,19,21,32,33] or strongly imbalanced [22] or immiscible two-species Bose-Einstein condensates (BECs) [10]. Further, in the aforementioned works, no systematic analysis has been done varying the intercomponent interaction.

In this work, we fill the gap by studying the dipole modes of a tunable ^{41}K - ^{87}Rb bosonic mixture confined in a harmonic trap. We induce the center-of-mass (CM) oscillations of both atomic species and, focusing on the linear response regime, we investigate their coupled dynamics. We measure the frequencies and the composition of the mixed dipole modes as a function of the interspecies interaction, from the weakly interacting to the strongly attractive regime, even beyond the mean-field collapse. For sufficiently strong interactions, we observe that the two condensates almost move as one. In this regime, we directly explore the role of the population imbalance and find that the dipole dynamics is governed by the in-phase mode whose frequency depends on the bare trap frequencies and the population imbalance. The experimental results are in good agreement with numerical simulations performed by solving two coupled Gross-Pitaevskii (GP) equations. We also discuss a simple

---

*burchianti@lens.unifi.it

model, based on the Ehrenfest theorem, which captures the main features of the dipole dynamics.

II. SYSTEM PREPARATION

We prepare binary condensates of ^{41}K and ^{87}Rb, following the methods described in Refs. [34,35]. Briefly, we start by loading both atomic species in a hybrid potential, consisting of a magnetic quadrupole plus a dimple laser beam. Here, ^{87}Rb is evaporatively cooled, while ^{41}K is cooled by thermal contact with ^{87}Rb. The cooling sequence ends with the production of a degenerate mixture, with both species in the $|F = 1, m_F = 1\rangle$ hyperfine ground state, in a purely optical potential. The final trap is formed by the dimple beam and an auxiliary beam, crossing at $45°$ in the horizontal plane. The typical condensate atom number $N_1 + N_2$ (hereafter we use the notation $1 \rightarrow {}^{41}$K and $2 \rightarrow {}^{87}$Rb) is 3×10^5 and the species population imbalance, $\alpha = N_1/N_2$, is adjusted by controlling the number of ^{41}K and ^{87}Rb atoms that are initially loaded in the hybrid trap [36].

The interspecies scattering length a_{12} is magnetically tuned by the Feshbach field, an homogeneous magnetic field B_z, directed along the vertical $\hat{z}$ axis (aligned antiparallel to gravity). In the range where B_z is varied, the intraspecies scattering lengths are both positive and almost constant: $a_{11} = 62a_0$ [37] $a_{22} = 100.4a_0$ [38]. We start the experiment with vanishing interspecies interactions by setting B_z close to 72 G, in correspondence of the zero-crossing point ($a_{12} = 0$) between two interspecies Feshbach resonances at 39 G and 79 G [39].

The trapping potential minima of ^{41}K, z_1^0, and ^{87}Rb, z_2^0, are vertically shifted due to the different harmonic trap frequencies. In order to overlap the two minima, we compensate the differential sag with a vertical magnetic field gradient b_z, taking advantage of the different magnetic moments of ^{41}K and ^{87}Rb in the B_z range [35]. The gradient is adiabatically ramped to -16.6 G/cm, ensuring $z_1^0 \simeq z_2^0$. Then, B_z is linearly varied in 20 ms from the zero-crossing to the target value of a_{12} and, finally, the dipole dynamics is started by increasing b_z up to -14.6 G/cm in about 1 ms. This changes the positions of the trapping minima along $\hat{z}$ by $\Delta_1 \simeq 2\,\mu$m and $\Delta_2 \simeq 1\,\mu$m, triggering the dipole dynamics.

The trap shifts are chosen as a compromise between the contrasting requirements of small perturbations and an acceptable signal-to-noise ratio of the recorded oscillations. It is worth noticing that for the typical in-trap amplitude oscillations, used in this work, the maximum relative velocity between the two superfluids remains below the sum of their sound velocities. This represents a necessary condition for preventing the emergence of dissipation [14,40,41].

For zero a_{12}, the measured trapping frequencies are $(\omega_{x,1}, \omega_{y,1}, \omega_{z,1}) \simeq 2\pi \times (65, 190, 185)$ Hz for ^{41}K and $(\omega_{x,2}, \omega_{y,2}, \omega_{z,2}) \simeq 2\pi \times (45, 140, 135)$ Hz for ^{87}Rb. Since the trap frequencies are very sensitive to the alignment of the trap beams, they are recorded daily and used as a normalization factor for the dipole mode frequencies observed for $a_{12} \neq 0$. Once the dipole dynamics is excited, the two condensates are held for a variable time in the optical dipole potential, then they are released from the trap and allowed to expand. After a time-of-flight (TOF) $t_{TOF} = 35$ (38) ms, we set $B_z = 0$ and record the ^{41}K (^{87}Rb) density distribution in

the yz plane by absorption imaging [42]. The effect of the interspecies interactions during the expansion is minimized by extinguishing b_z 1 ms later than the optical potential. The corresponding species-selective magnetic force contributes to separate the two falling condensates. From the density distribution we extract the vertical displacements of the CM positions of ^{41}K and ^{87}Rb, $\Delta z_{CM,1}$ and $\Delta z_{CM,2}$.

The atom number is calculated from the size and optical depth of the atomic clouds and is calibrated by matching the TOF expansion of single-species BECs with the expected theoretical behavior [43]. We estimate an uncertainty in the atomic number correction of 20% and 10% for ^{41}K and ^{87}Rb, respectively.

III. COUPLED DIPOLE OSCILLATIONS

As common to many physical situations, two coupled oscillators exhibit two oscillation modes whose frequencies differ from the natural frequencies of the uncoupled systems and whose amplitudes generally depend on the initial conditions. In our case, the two oscillating BECs are coupled by the coupling constant g_{12} which is proportional to a_{12}: $g_{ij} = 2\pi\hbar^2 a_{ij}/m_{ij}$, with $m_{ij} = m_i m_j/(m_i + m_j)$ $(i, j = 1, 2)$.

A simple theoretical description of the present system can be obtained by means of the Ehrenfest theorem, or, equivalently, of the sum-rules approach, as discussed in the Appendix. In this case the frequencies $\omega_{\pm}$ of the two modes have the analytical expression given by Eq. (A7), and their shifts from the bare trap frequencies ($\omega_{z,1}$ and $\omega_{z,2}$), for a given mixture, are fixed by g_{12} and by the equilibrium density distributions. In particular, in the attractive (repulsive) regime the eigenmode frequencies are raised (lowered) by the interspecies interactions. Analyzing the eigenvectors of the matrix Eq. (A6), one can gain information on the relative phase of the two modes [44]. More specifically, in the attractive regime, the low-energy mode corresponds to the in-phase oscillations of the two condensates, while the high-energy mode corresponds to the out-of-phase ones. The situation is reversed in the repulsive regime, where the in-phase dynamics occurs for the high-energy mode.

However, it is worth noticing that since this model relies on the knowledge of the equilibrium configuration only, its predictions may become inaccurate if during the dynamics the shape of density distributions deviates significantly from the initial one, (i.e., when the evolution of each condensate cannot be described by a rigid translation). Therefore, in order to have a more accurate description of the observed oscillations, we perform full dynamical GP simulations (see Appendix).

In Fig. 1(a) we show the experimental CM shifts, $\Delta z_{CM,1}$ and $\Delta z_{CM,2}$, as a function of the in-trap time for an attractive mixture with $a_{12} = -(30.7 \pm 1.2)a_0$, $N_1 \simeq 7 \times 10^4$, and $\alpha \in [0.4, 0.6]$ [45]. The variation range of α is due to fluctuations in the ^{41}K and ^{87}Rb atom numbers during the measurement. We observe that, in this regime, the ^{87}Rb dipole dynamics is dominated by a single mode with frequency ω_-, while the ^{41}K one clearly shows two distinct modes with frequencies ω_- and ω_+, as clearly shown by the Fourier transform of the data [see Fig. 1(b)]. The measurements are well reproduced by the corresponding GP simulations (continuous lines) where, by assuming that the interaction effects during the
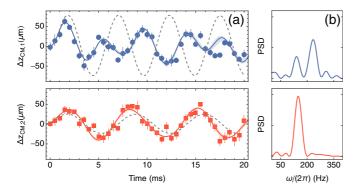
FIG. 1. (a) Oscillations of $\Delta z_{CM,1}$ (blue circle, upper panel) and $\Delta z_{CM,2}$ (red squares, lower panel) in the attractive regime for $a_{12} = -(30.7 \pm 1.2)a_0$. The vertical CM positions, extracted from the density profiles, are measured after a TOF expansion of 35 ms (upper panel) and 38 ms (lower panel) for ^{41}K and ^{87}Rb, respectively. Error bars denote standard deviation of mean over five independent measurements. The continuous lines are the corresponding GP simulations where all parameters are fixed to the experimental ones, with the exception of the initial phases, which are fitting parameters. The continuous lines are obtained for $\alpha = 0.5$ and the shaded area corresponds to $0.4 \leqslant \alpha \leqslant 0.6$. As a reference, GP simulations for the two atomic species at $a_{12} = 0$ are also displayed as gray dashed curves. (b) Power spectral density (PSD) of the ^{41}K (upper panel) and ^{87}Rb oscillation data (lower panel).

TOF are negligible, the expansion is obtained via the mapping $\Delta z_{CM}(t + t_{TOF}) = \Delta z_{CM}(t) + t_{TOF} v_{CM}(t)$ (v_{CM} being the vertical CM velocity at time t). In Fig. 1(a) we also report, as a reference, the GP simulations for $a_{12} = 0$ (dashed lines). The comparison with the latter shows that the frequencies of both modes are upshifted by the mean-field attraction, as expected (see Appendix).

IV. GENERAL RESULTS AND DISCUSSION

We have systematically investigated the dipole dynamics of the ^{41}K - ^{87}Rb mixture, varying the interaction coupling from the weakly to the strongly attractive side. We restrict our analysis to this interaction range in order to remain in the linear response regime and to avoid the counterflow instability [41]. Indeed, repulsive interactions increase the relative velocity between the two condensates by pushing them apart, and, at the same time, they are expected to lower the value of the critical velocity associated with the relative motion [14].

We measure both the frequencies (ω_-, ω_+) and the amplitudes (A_-, A_+) [46] of the dipole eigenmodes as a function of a_{12}. These quantities are extracted by fitting the CM positions of the two condensates with

$$\Delta z_{CM} = \sum_{\kappa = \pm} A_\kappa e^{-t/\tau_\kappa} \sin(\omega_\kappa t + \phi_\kappa). \qquad (1)$$

The decay times (τ_+, τ_-) are introduced to take into account damping effects which may emerge due to reasons both external and intrinsic to the dipole dynamics, as discussed in the following.

We initially consider the case of slightly imbalanced mixtures, with $\alpha \in [0.32, 0.84]$, $N_1 \simeq 7 \times 10^4$ for $-80a_0 < a_{12} \leqslant 9a_0$, and $N_1 \simeq 5 \times 10^4$ for $a_{12} \leqslant -80a_0$. In Fig. 2, we show the
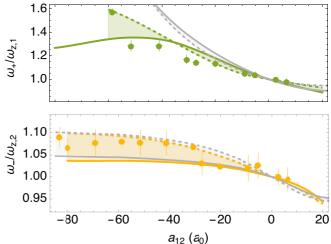

FIG. 2. Normalized eigenmode frequencies of a ^{41}K - ^{87}Rb mixture as a function of a_{12}: The frequency of the high-energy eigenmode is obtained by fitting the ^{41}K oscillation (green circles, upper panel); the frequency of the low-energy eigenmode is obtained by fitting the ^{87}Rb oscillation or, whenever possible (see text), it is given by the mean of the values obtained by fitting the motion of both atomic species (yellow circles, lower panel). The colored areas indicate the GP numerical predictions corresponding to the maximum experimental variation of α: Dashed colored lines for $\alpha = 0.84$ and continuous lines for $\alpha = 0.32$. For comparison, the corresponding results from Eq. (A7) are also reported as gray lines: Dashed for $\alpha = 0.84$ and continuous for $\alpha = 0.32$.

frequencies of the high- and low-energy eigenmodes, respectively normalized to $\omega_{z,1}$ and $\omega_{z,2}$, versus a_{12}. On the attractive (repulsive) side, both ω_+ and ω_- are up (down) shifted and this shift increases with the strength of the interspecies interaction. The experimental data are compared to the results of the GP simulations (colored regions) and to the predictions of the Ehrenfest theorem in Eq. (A7) (gray regions). In addition, in Fig. 3 we show the amplitudes A_+ and A_- extracted from the CM oscillations of both ^{41}K (upper panel) and ^{87}Rb (lower panel). The amplitude of each condensate is normalized to the corresponding amplitude measured at $a_{12} = 0$ (that is, A_1 for ^{41}K and A_2 for ^{87}Rb). For weak interspecies interactions, the ^{41}K oscillations are characterized only by the high-energy eigenmode, with relative amplitude A_+/A_1 (data points). As the attractive interaction increases, the low-energy eigenmode, with relative amplitude A_-/A_1 (data points), starts to appear and becomes dominant in the strongly attractive regime. On the contrary, the ^{87}Rb oscillation is always dominated by the low-energy eigenmode and only the relative amplitude A_-/A_2 can be measured. This result can be intuitively explained by considering the two opposite limits: at $a_{12} = 0$, the low-energy eigenmode is the Rb unperturbed oscillation; in the strongly attractive case, the two condensates move together and their position nearly coincides with the ^{87}Rb one, due to the larger atomic mass and atom number. Therefore, in the case of ^{87}Rb only the oscillation frequency is slightly affected by the mean-field attraction.

In order to reproduce the experimental results we perform corresponding GP simulations. The colored areas in Figs. 2
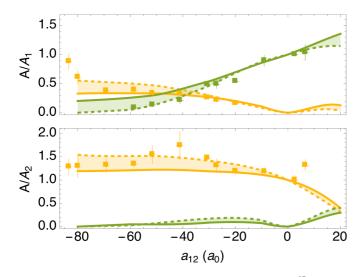
FIG. 3. Normalized eigenmode amplitudes of a ^{41}K - ^{87}Rb mixture as a function of a_{12}. Upper panel: Experimental amplitudes of the low-energy (yellow squares) and high-energy (green squares) eigenmodes of ^{41}K. Lower panel: Experimental amplitude of the low-energy (yellow squares) eigenmode of ^{87}Rb. The colored areas indicate the GP numerical predictions corresponding to the maximum variation of α during the measurements: The dashed line is for $\alpha = 0.84$, while the continuous one is for $\alpha = 0.32$. In the lower panel the green area shows the predicted amplitude of the ^{87}Rb high-energy egeinmode which cannot be experimentally resolved.

and 3 show the numerical predictions obtained by considering the maximum variation of α during the measurements: the continuous line corresponds to $\alpha = 0.32$ and the dashed one to $\alpha = 0.84$. The agreement between GP theory and the experiment is good in the full range of explored interactions. For completeness, we also show in Fig. 2 the eigenmode frequencies calculated with Eq. (A7). Approaching the strongly attractive side, we see that only the lower frequency mode, corresponding to the in-phase motion of the two condensates, is well reproduced by the Ehrenfest model.

Even for weak couplings ($a_{12} < -10a_0$), we measure a nonnegligible damping of the high-energy dipole mode with a decay time τ_+ of about 20 ms. This effect, also observable in the GP simulations, is the result of nonlinear coupling to other collective modes for large enough excitations. We also observe a decay of the dipole oscillations, depending on their amplitude, when $a_{12} = 0$, due to the anharmonicity of the trap potential away from its minimum. However, in this case the decay time is of about 200 ms for trap shifts of the order of $2\,\mu$m, substantially longer than τ_+.

For sufficiently strong interactions, namely, for $a_{12} < -70a_0$, we observe that the two condensates oscillate in unison, with the same frequency and amplitude. In this limit, the eigenmode frequency ω_- tends to the value

$$\omega_- = \sqrt{\frac{N_1 m_1 \omega_{z,1}^2 + N_2 m_2 \omega_{z,2}^2}{N_1 m_1 + N_2 m_2}}. \qquad (2)$$

It is worth noticing that this expression depends only on the bare trap frequencies and on the total masses $N_i m_i$ of the two components.
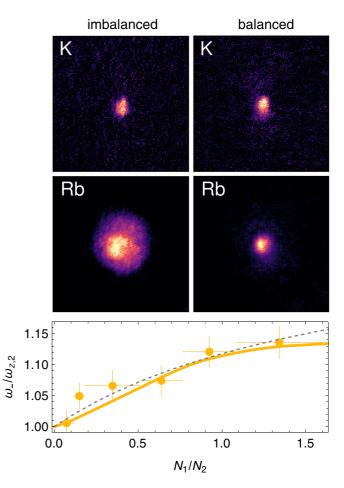

FIG. 4. Upper panel: Absorption images of imbalanced and balanced dual-species BEC, in the strongly attractive regime, for $a_{12} = -(83.4 \pm 1.2)a_0$. Images are taken after 35 ms of TOF for ^{41}K and 38 ms for ^{87}Rb; $N_1 = (4.7 \pm 1.0) \times 10^4$ and $N_2 = (3.4 \pm 0.3) \times 10^5$ in the imbalanced case, and $N_1 = (4.8 \pm 1.0) \times 10^4$ and $N_2 = (5.5 \pm 0.6) \times 10^4$, in the balanced case. Lower panel: Normalized frequency of the low-energy eigenmode as a function of the species population imbalance α for $a_{12} = -(83.4 \pm 1.2)a_0$. The horizontal error bars correspond to the binning intervals of α values. The systematic uncertainty due to the atom number calibration mentioned in the text corresponds to multiplying all α values for a scaling factor of (1.0 ± 0.22). The continuous line is the result of GP simulations and the gray dashed line is the solution of Eq. (2).

We verify the accuracy of Eq. (2) in the strongly interacting regime for $a_{12} = -(83.4 \pm 1.2)a_0$, where the mixture is stabilized against the mean-field collapse by quantum fluctuations [47], i.e., for $g_{12} < -\sqrt{g_{11}g_{22}}$ (for our mixture the critical point corresponds to $a_{12}^c = -73.6a_0$). To this end, we measure the low-energy eigenmode frequency once the species population imbalance spans a wider range, for $\alpha \in [0.07, 1.34]$. In Fig. 4, we show the corresponding values of ω_- as a function of α. The experimental data points are compared with the results of both the GP simulations including the Lee-Huang-Yang correction (continuous line, see Appendix) and Eq. (2) (dashed line). The frequency shift from the bare value $\omega_{z,2}$ decreases by decreasing α and eventually tends to $\omega_{z,2}$ when $\alpha \ll 1$.

Because the dipole dynamics is insensitive to the presence of liquid droplets, we probe their possible existence using TOF detection since, differently from the unbound gas component, droplets do not expand after the trap removal. Following the system evolution up to $t_{\text{TOF}} = 25$ ms [48], we observe that, in the same conditions of Fig. 4, i.e., for $a_{12} = -83.4a_0$, both atomic species expand, even if the atom number exceeds the critical value for droplet formation [35]. This effect can be ascribed to the fact that the system is prepared in a configuration far from the equilibrium one in free space. We verified that stable droplets form by further increasing the interspecies attraction. However, such an increase implies a substantial reduction of the mixture lifetime, due to the enhancement of three-body losses. This hinders the study of the in-trap dynamics in this range of parameters. We conclude that the production of long-lived droplet states requires a trap geometry matching the droplet size in free space, which is out the scope of the present work [49,50].

V. CONCLUSIONS

We have studied the coupled dipole dynamics of a binary condensate by exploiting an asymmetric bosonic mixture, where the two components have different masses and experience different trapping potentials. In particular, we have investigated the dipole excitations of the two condensates as a function of their mutual coupling, exploring different regions of the mixture phase diagram. In the weakly interacting regime, where the mixture is miscible, we have excited both the in-phase and out-of-phase dipole modes, both observable in the CM oscillations of component 1, and measured their dependence on the intercomponent interaction. We find that the frequencies of both eigenmodes are shifted by the coupling, different from the case of symmetric spin mixtures, where the in-phase dipole frequency always matches the trap frequency. Further, we have extended our analysis to the strongly attractive regime, where the mixture is stabilized by quantum fluctuations. Approaching this region, the most significant features are the dominance of the in-phase dynamics and the unison motion of the two condensates. In this limit, the dipole frequency is determined only by the bare trap frequencies and the total masses of the two components. Our findings provide a solid ground for future experimental studies aimed at exploring the coupled dynamics of bosonic mixtures in different regimes, even beyond the linear limit, such as in the presence of dissipation or in proximity of a phase transition. Further extensions of our work could also include the exploration of higher-order excitations, which may be useful for probing quantum fluctuations [51], exotic matter states [52], and topological structures [53] in multicomponent superfluids.

APPENDIX: THEORETICAL MODEL

The system under study can be described by two coupled GP equations of the form ($i, j = 1, 2$),

$$i\hbar\partial_t\psi_i(\boldsymbol{r}, t) = \left[-\frac{\hbar^2}{2m_i}\nabla^2 + V_i^{\text{tot}}(\boldsymbol{r}, t)\right]\psi_i(\boldsymbol{r}, t), \quad \text{(A1)}$$

where V_i^{tot} represents the total mean-field potential acting on the species $i(\neq j)$,

$$V_i^{\text{tot}}(\boldsymbol{r}, t) = V_i^{ho}(\boldsymbol{r}) + g_{ii}n_i(\boldsymbol{r}, t) + g_{ij}n_j(\boldsymbol{r}, t), \quad \text{(A2)}$$

with $n_i(\boldsymbol{r}, t) \equiv |\psi_i(\boldsymbol{r}, t)|^2$ and $\int n_i = N_i$. The structure of the (collective) dipole modes along z can be obtained by means of the Ehrenfest theorem [54], namely,

$$\frac{d^2}{dt^2}\langle z\rangle_i = -\frac{1}{m_i}\langle\partial_z V_i^{\text{tot}}\rangle_i. \quad \text{(A3)}$$

Then, by defining $\delta z_i(t) \equiv \langle z\rangle_i(t)$ it is straightforward to get [55]

$$\ddot{\delta z}_i(t) = -\omega_i^2\delta z_i(t) - \frac{g_{ij}}{m_i N_i}\int n_i\partial_z n_j. \quad \text{(A4)}$$

In the *limit of small oscillations*, the integral in the last term can be evaluated explicitly by assuming that the densities translate rigidly, $n_i(z, t) = n_{0i}[z - \delta z_i(t)]$, and using the following approximation: $n_i(z, t) \simeq n_{0i}(z) - \partial_z n_{0i}(z)\delta z_i(t)$ (for ease of notation, we have omitted the dependence on the transverse coordinates x and y). Within these approximations, by defining $I \equiv \int \partial_z n_{01}\partial_z n_{02}$ and $\eta_i \equiv g_{12}I/(m_i N_i)$, Eq. (A4) can be recast in matrix form as

$$\ddot{\delta z} = -M\delta z, \quad \text{with } \delta z \equiv \begin{pmatrix} \delta z_1 \\ \delta z_2 \end{pmatrix} \quad \text{(A5)}$$

and

$$M = \begin{pmatrix} \omega_1^2 - \eta_1 & \eta_1 \\ \eta_2 & \omega_2^2 - \eta_2 \end{pmatrix}. \quad \text{(A6)}$$

The frequencies $\omega_\pm$ of the two dipole modes are obtained from the eigenvalues of M, namely,

$$\omega_\pm^2 = \frac{1}{2}\sum_{i=1}^{2}(\omega_i^2 - \eta_i)$$

$$\pm\sqrt{\left[\sum_{i=1}^{2}(\omega_i^2 - \eta_i)/2\right]^2 + (\omega_1^2\eta_2 + \omega_2^2\eta_1) - \omega_1^2\omega_2^2}. \quad \text{(A7)}$$

From the above equation one can easily see that in the attractive regime ($g_{12} < 0$) the two modes are upshifted with respect to the bare trapping frequencies ω_1 and ω_2 of the two condensates, while in the repulsive ($g_{12} > 0$) regime they are downshifted. It is also worth noticing that these frequencies are fixed by the equilibrium configuration of the system (i.e., the ground state in the same harmonic potential in which the evolution takes place) through the integral

$I = \int \partial_z n_{01} \partial_z n_{02}$ [56], as in the case of the sum-rules approach (see, e.g., Refs. [26,57]). Indeed, it can be shown that the two approaches are equivalent [44].

For a general description, beyond the linear regime of small oscillations and of the rigid displacement ansatz [see below Eq. (A4)], we perform dynamical simulations of the full GP equation [Eq. (A1)] to take into account the deformations of the density profiles during the evolution of the system. In addition, since at the mean-field level the mixture becomes unstable against collapse at $g_{12} = -\sqrt{g_{11}g_{22}}$, in the strongly attractive regime we also include the Lee-Huang-Yang (LHY) correction [58] that accounts for the stabilizing effect of quantum fluctuations [47]. In particular, in Eq. (A1) we include a term $V_{\text{LHY},i} \equiv \partial \mathcal{E}_{\text{LHY}}/\partial n_i$, where the LHY energy density $\mathcal{E}_{\text{LHY}}$ can be written in the form [59,60]

$$\mathcal{E}_{\text{LHY}} = \frac{8}{15\pi^2\hbar^3}\left(g_{11}n_1m_1^{3/5} + g_{22}n_2m_2^{3/5}\right)^{5/2}. \quad (A8)$$

[1] M. Iskin and C. A. R. Sá de Melo, Two-band superfluidity from the BCS to the BEC limit, Phys. Rev. B **74**, 144517 (2006).

[2] H. Tajima, Y. Yerin, A. Perali, and P. Pieri, Enhanced critical temperature, pairing fluctuation effects, and BCS-BEC crossover in a two-band Fermi gas, Phys. Rev. B **99**, 180503(R) (2019).

[3] Y. Yerin, H. Tajima, P. Pieri, and A. Perali, Coexistence of giant Cooper pairs with a bosonic condensate and anomalous behavior of energy gaps in the BCS-BEC crossover of a two-band superfluid Fermi gas, Phys. Rev. B **100**, 104528 (2019).

[4] L. Salasnich, A. A. Shanenko, A. Vagov, J. A. Aguiar, and A. Perali, Screening of pair fluctuations in superconductors with coupled shallow and deep bands: A route to higher-temperature superconductivity, Phys. Rev. B **100**, 064510 (2019).

[5] D. O. Edwards, D. F. Brewer, P. Seligman, M. Skertic, and M. Yaqub, Solubility of He³ in Liquid He⁴ at 0°K, Phys. Rev. Lett. **15**, 773 (1965).

[6] A. F. Andreev and E. P. Bashkin, Three-velocity hydrodynamics of superfluid solutions, Sov. Phys. JETP **42**, 164 (1975).

[7] M. A. Alpar, S. A. Langer, and J. A. Sauls, Rapid postglitch spin-up of the superfluid core in pulsars, Astrophys. J. **282**, 533 (1984).

[8] N. Andersson, G. L. Comer, and R. Prix, Are Pulsar Glitches Triggered by a Superfluid Two-Stream Instability?, Phys. Rev. Lett. **90**, 091101 (2003).

[9] D. N. Kobyakov and C. J. Pethick, Two-component superfluid hydrodynamics of neutron star cores, Astrophys. J. **836**, 203 (2017).

[10] G. Modugno, M. Modugno, F. Riboli, G. Roati, and M. Inguscio, Two Atomic Species Superfluid, Phys. Rev. Lett. **89**, 190404 (2002).

[11] I. Ferrier-Barbut, M. Delehaye, S. Laurent, A. T. Grier, M. Pierce, B. S. Rem, F. Chevy, and C. Salomon, A mixture of Bose and Fermi superfluids, Science **345**, 1035 (2014).

[12] R. Roy, A. Green, R. Bowler, and S. Gupta, Two-Element Mixture of Bose and Fermi Superfluids, Phys. Rev. Lett. **118**, 055301 (2017).

[13] V. P. Mineev, The theory of the solution of two near-ideal Bose gases, Sov. Phys. JETP **40**, 132 (1974).

[14] C. K. Law, C. M. Chan, P. T. Leung, and M.-C. Chu, Critical velocity in a binary mixture of moving Bose condensates, Phys. Rev. A **63**, 063612 (2001).

[15] H. Pu and N. P. Bigelow, Collective Excitations, Metastability, and Nonlinear Response of a Trapped Two-Species Bose-Einstein Condensate, Phys. Rev. Lett. **80**, 1134 (1998).

[16] P. Öhberg and S. Stenholm, Coupled eigenmodes in a two-component Bose-Einstein condensate, J. Phys. B: At. Mol. Opt. Phys. **32**, 1959 (1999).

[17] I. Vidanović, N. J. van Druten, and M. Haque, Spin modulation instabilities and phase separation dynamics in trapped two-component Bose condensates, New J. Phys. **15**, 035008 (2013).

[18] D. S. Hall, M. R. Matthews, J. R. Ensher, C. E. Wieman, and E. A. Cornell, Dynamics of Component Separation in a Binary Mixture of Bose-Einstein Condensates, Phys. Rev. Lett. **81**, 1539 (1998).

[19] P. Maddaloni, M. Modugno, C. Fort, F. Minardi, and M. Inguscio, Collective Oscillations of Two Colliding Bose-Einstein Condensates, Phys. Rev. Lett. **85**, 2413 (2000).

[20] M. Egorov, B. Opanchuk, P. Drummond, B. V. Hall, P. Hannaford, and A. I. Sidorov, Measurement of s-wave scattering lengths in a two-component Bose-Einstein condensate, Phys. Rev. A **87**, 053614 (2013).

[21] T. Bienaimé, E. Fava, G. Colzi, C. Mordini, S. Serafini, C. Qu, S. Stringari, G. Lamporesi, and G. Ferrari, Spin-dipole oscillation and polarizability of a binary Bose-Einstein condensate near the miscible-immiscible phase transition, Phys. Rev. A **94**, 063652 (2016).

[22] K. E. Wilson, A. Guttridge, I. Kang Liu, J. Segal, T. P. Billam, N. G. Parker, N. P. Proukakis, and S. L. Cornish, Dynamics of a degenerate Cs-Yb mixture with attractive interspecies interactions, Phys. Rev. Res. **3**, 033096 (2021).

[23] W. Kohn, Cyclotron resonance and de Haas-van Alphen oscillations of an interacting electron gas, Phys. Rev. **123**, 1242 (1961).

[24] E. Fava, T. Bienaimé, C. Mordini, G. Colzi, C. Qu, S. Stringari, G. Lamporesi, and G. Ferrari, Observation of Spin Superfluidity in a Bose Gas Mixture, Phys. Rev. Lett. **120**, 170401 (2018).

[25] X.-C. Yao, H.-Z. Chen, Y.-P. Wu, X.-P. Liu, X.-Q. Wang, X. Jiang, Y. Deng, Y.-A. Chen, and J.-W. Pan, Observation of Coupled Vortex Lattices in a Mass-Imbalance Bose and Fermi Superfluid Mixture, Phys. Rev. Lett. **117**, 145301 (2016).

[26] T. Miyakawa, T. Suzuki, and H. Yabu, Sum-rule approach to collective oscillations of a boson-fermion mixed condensate of alkali-metal atoms, Phys. Rev. A **62**, 063613 (2000).

[27] A. Banerjee, Collective oscillations of a Bose-Fermi mixture: Effect of unequal masses of Bose and Fermi particles, Phys. Rev. A **76**, 023611 (2007).

[28] T. Maruyama and G. F. Bertsch, Dipole oscillations in Bose-Fermi mixtures in the time-dependent Gross-Pitaevskii and Vlasov equations, Phys. Rev. A **77**, 063611 (2008).

[29] J. J. Kinnunen and G. M. Bruun, Induced interactions in a superfluid Bose-Fermi mixture, Phys. Rev. A **91**, 041605(R) (2015).

[30] Y.-P. Wu, X.-C. Yao, X.-P. Liu, X.-Q. Wang, Y.-X. Wang, H.-Z. Chen, Y. Deng, Y.-A. Chen, and J.-W. Pan, Coupled dipole os-

cillations of a mass-imbalanced Bose-Fermi superfluid mixture, Phys. Rev. B **97**, 020506(R) (2018).

[31] W. Wen, Y. Wang, and J. Wang, Collective oscillation modes of a superfluid Bose-Fermi mixture, New J. Phys. **21**, 093011 (2019).

[32] C. Hamner, J. J. Chang, P. Engels, and M. A. Hoefer, Generation of Dark-Bright Soliton Trains in Superfluid-Superfluid Counterflow, Phys. Rev. Lett. **106**, 065302 (2011).

[33] J.-Y. Zhang, S.-C. Ji, Z. Chen, L. Zhang, Z.-D. Du, B. Yan, G.-S. Pan, B. Zhao, Y.-J. Deng, H. Zhai, S. Chen, and J.-W. Pan, Collective Dipole Oscillations of a Spin-Orbit Coupled Bose-Einstein Condensate, Phys. Rev. Lett. **109**, 115301 (2012).

[34] C. D'Errico, A. Burchianti, M. Prevedelli, L. Salasnich, F. Ancilotto, M. Modugno, F. Minardi, and C. Fort, Observation of quantum droplets in a heteronuclear bosonic mixture, Phys. Rev. Res. **1**, 033155 (2019).

[35] A. Burchianti, C. D'Errico, M. Prevedelli, L. Salasnich, F. Ancilotto, M. Modugno, F. Minardi, and C. Fort, A dual-species Bose-Einstein condensate with attractive interspecies interactions, Condens. Matter **5**, 21 (2020).

[36] The production of degenerate mixtures with ^{41}K as the majority species is hindered by the ineffectiveness of sympathetic cooling observed once we decrease the starting number of ^{87}Rb atoms.

[37] A. Simoni, private communication.

[38] A. Marte, T. Volz, J. Schuster, S. Dürr, G. Rempe, E. G. M. van Kempen, and B. J. Verhaar, Feshbach Resonances in Rubidium 87: Precision Measurement and Analysis, Phys. Rev. Lett. **89**, 283202 (2002).

[39] G. Thalhammer, G. Barontini, L. De Sarlo, J. Catani, F. Minardi, and M. Inguscio, Double Species Bose-Einstein Condensate with Tunable Interspecies Interactions, Phys. Rev. Lett. **100**, 210402 (2008).

[40] Y. Castin, I. Ferrier-Barbut, and C. Salomon, La vitesse critique de landau d'une particule dans un superfluide de fermions, C. R. Phys. **16**, 241 (2015).

[41] M. Abad, A. Recati, S. Stringari, and F. Chevy, Counter-flow instability of a quantum mixture of two superfluids, Eur. Phys. J. D **69**, 126 (2015).

[42] The different TOF between ^{41}K and ^{87}Rb is due to the technical limitation of the CCD camera, once operated in the double-shot mode.

[43] Y. Castin and R. Dum, Bose-Einstein Condensates in Time Dependent Traps, Phys. Rev. Lett. **77**, 5315 (1996).

[44] C. Fort and M. Modugno, Dipole modes of a trapped bosonic mixture: Fate of the sum-rule approach, Phys. Rev. A **106**, 043311 (2022).

[45] The vertical BEC radii are $\sim 4.5 \mu$m and $\sim 5 \mu$m for ^{41}K and ^{87}Rb, respectively.

[46] We remark that the frequencies $\omega_\pm$ are intrinsic properties of the system, whereas the amplitudes $A_\pm$ also depend on the protocol employed to excite the dynamics.

[47] D. S. Petrov, Quantum Mechanical Stabilization of a Collapsing Bose-Bose Mixture, Phys. Rev. Lett. **115**, 155302 (2015).

[48] For larger TOF the atoms exit, under the effect of gravity, the region where the Feshbach field is spatially homogeneous [34].

[49] G. Ferioli, G. Semeghini, S. Terradas-Briansó, L. Masi, M. Fattori, and M. Modugno, Dynamical formation of quantum droplets in a ^{39}K mixture, Phys. Rev. Res. **2**, 013269 (2020).

[50] Z. Guo, F. Jia, L. Li, Y. Ma, J. M. Hutson, X. Cui, and D. Wang, Lee-Huang-Yang effects in the ultracold mixture of ^{23}Na and ^{87}Rb with attractive interspecies interactions, Phys. Rev. Res. **3**, 033247 (2021).

[51] T. G. Skov, M. G. Skou, N. B. Jørgensen, and J. J. Arlt, Observation of a Lee-Huang-Yang Fluid, Phys. Rev. Lett. **126**, 230404 (2021).

[52] H. Hu and X.-J. Liu, Collective excitations of a spherical ultradilute quantum droplet, Phys. Rev. A **102**, 053303 (2020).

[53] A. Wolf, P. Boegel, M. Meister, A. Balaž, N. Gaaloul, and M. A. Efremov, Shell-shaped Bose-Einstein condensates based on dual-species mixtures, Phys. Rev. A **106**, 013309 (2022).

[54] P. Ehrenfest, Bemerkung über die angenäherte Gültigkeit der klassischen Mechanik innerhalb der Quantenmechanik, Z. Phys. **45**, 455 (1927).

[55] We have used the fact that $\int_i \partial_z n_i = \int (n_i^2)/2 \equiv 0$ because of the vanishing boundary conditions.

[56] The equilibrium densities $n_{0i}(\boldsymbol{x})$ have to be computed numerically by minimizing the GP energy functional [61] corresponding to Eq. (A1).

[57] S. Stringari, Collective Excitations of a Trapped Bose-Condensed Gas, Phys. Rev. Lett. **77**, 2360 (1996).

[58] T. D. Lee, K. Huang, and C. N. Yang, Eigenvalues and eigenfunctions of a Bose system of hard spheres and its low-temperature properties, Phys. Rev. **106**, 1135 (1957).

[59] F. Ancilotto, M. Barranco, M. Guilleumas, and M. Pi, Self-bound ultradilute Bose mixtures within local density approximation, Phys. Rev. A **98**, 053623 (2018).

[60] F. Minardi, F. Ancilotto, A. Burchianti, C. D'Errico, C. Fort, and M. Modugno, Effective expression of the Lee-Huang-Yang energy functional for heteronuclear mixtures, Phys. Rev. A **100**, 063636 (2019).

[61] L. P. Pitaevskii and S. Stringari, *Bose-Einstein Condensation and Superfluidity* (Oxford University Press, New York, 2016).